

# MerR Cross-Links to the $\alpha$ , $\beta$ , and $\sigma^{70}$ Subunits of RNA Polymerase in the Preinitiation Complex at the *merTPCAD* Promoter<sup>†</sup>

Resham D. Kulkarni and Anne O. Summers\*

Department of Microbiology, University of Georgia, Athens, Georgia 30602

Received November 30, 1998; Revised Manuscript Received January 19, 1999

**ABSTRACT:** MerR, the metalloregulator of the mercury resistance (*mer*) operon, binds the operator (*merO*) between  $-10$  and  $-35$  of the *merTPCAD* promoter ( $P_T$ ) and sequesters RNA polymerase (RNAP) in a closed complex. MerR represses  $P_T$  until Hg(II) induces it to unwind *merO* DNA and thus facilitate open complex formation. We used cross-linking to determine if direct contacts between MerR and RNAP also occur during this process. MerR cross-linked to the  $\alpha$ ,  $\beta$ , and  $\sigma^{70}$  subunits of RNAP alone, indicating stable contacts which were further stabilized upon forming the preinitiation complex at  $P_T$ . Hg(II) did not eliminate any of the MerR–RNAP cross-links but did increase the relative abundance of a MerR dimer conformer. Interference by MerR with self-cross-links among RNAP subunits and the formation of an electrophoretically stable association between MerR and RNAP also indicated MerR–RNAP interactions. This is the first evidence for stable physical contacts between MerR and RNAP and for a Hg(II)-induced allosteric change in MerR in the transcription-competent complex.

A major control point in the regulation of prokaryotic gene expression occurs at transcriptional initiation. Interactions between activators or repressors and one or more of the RNAP<sup>1</sup> subunits are integral to regulation of transcriptional initiation (1). Some activators also effect changes in the structure of DNA which can include DNA bending or looping (2).

MerR, the transcriptional regulator of the bacterial Hg(II) resistance (*mer*) operon, represses initiation from the overlapping promoters of the divergent *merTPCAD* transcript ( $P_T$ ) and that of its own gene *merR* ( $P_R$ ) (3). Both  $P_T$  and  $P_R$  have good  $-10$  and  $-35$   $\sigma^{70}$  recognition hexamers but deviate from consensus in that the hexamer spacing is 19 bp for  $P_T$  and 15 bp for  $P_R$  rather than the optimum  $17 \pm 1$  bp. Apo-MerR binds a dyadic operator site (*merO*) lying between the  $-10$  and  $-35$  of  $P_T$  (4–6) and bends the DNA ca.  $25^\circ$  (7). A predicted helix–turn–helix in the N-terminal domain of the 144 amino acid MerR mediates DNA binding (8, 9). Apo-MerR, bound to *merO*, also sequesters RNAP as a closed complex at  $P_T$  until Hg(II) induces formation of an open complex at  $P_T$ . MerR–Hg(II) continues to repress  $P_R$  (10–12). MerR–Hg(II) remains bound to the DNA (10, 11, 13, 14), but its affinity for DNA and the bends it induces in DNA may change (10–18). A key component of the activation process is a MerR–Hg(II)-effected underwinding of *merO* DNA which aligns the  $-10$  and  $-35$  optimally for RNAP to initiate transcription. (7, 15, 19). Thus, control of transcription at  $P_T$  and  $P_R$  includes three very unusual elements: (i) MerR operates from one binding site for both

repression and activation although the location of this site would be expected to serve only repression; (ii) MerR sequesters RNAP holoenzyme in a stable nontranscribing complex at  $P_T$  prior to addition of the inducer Hg(II) (“active repression”; 20, 21); and (iii) when Hg(II) is added, MerR underwinds the DNA ca.  $30^\circ$ , allowing RNAP to contact the  $-10$  region and begin transcription at  $P_T$ .

Are MerR’s manipulations of DNA all that is required to accomplish active repression and transcriptional activation or does MerR also engage in functional protein–protein interactions with RNAP itself in these processes? Genetic corroboration for a “DNA-manipulations-only” mechanism is provided by loss-of-activation mutations in MerR whose defects lie either in Hg(II) binding or in DNA underwinding; all of these mutants which bind DNA also sequester RNAP at  $P_T$  in vivo (8, 9, 14). However MerR–RNAP interactions were suggested by other MerR mutants that have normal Hg(II) and DNA binding abilities but are defective in either activation (8) or repression (22).

To test the hypothesis that protein–protein interactions play a role in transcriptional initiation at  $P_T$ , we previously examined mutations in *rpoD* and *rpoA* known to influence activator-specific initiation at other promoters (23). We found MerR-dependent effects of mutants in the extreme C-termini of  $\sigma^{70}$  and of  $\alpha$ . In work reported here, we assessed the potential for functional protein interactions using electrophoretic mobility shift assays (EMSA) and chemical cross-linking to observe associations between MerR and the subunits of RNAP. Our findings strongly implicate protein–protein interactions in transcriptional control of *mer* operon expression.

## EXPERIMENTAL PROCEDURES

**Purification of MerR.** C-Terminal His-tagged MerR was purified according to Zeng et al. (24).

<sup>†</sup> This work was supported by NIH Grant GM28211 to A.O.S.

\* Correspondence should be addressed to this author. Telephone: (706) 542-2669. Fax: (706) 542-6140. Email: summers@arches.uga.edu.

<sup>1</sup> Abbreviations: RNAP, RNA polymerase;  $P_T$ , *merTPCAD* promoter;  $P_R$ , *merR* promoter.

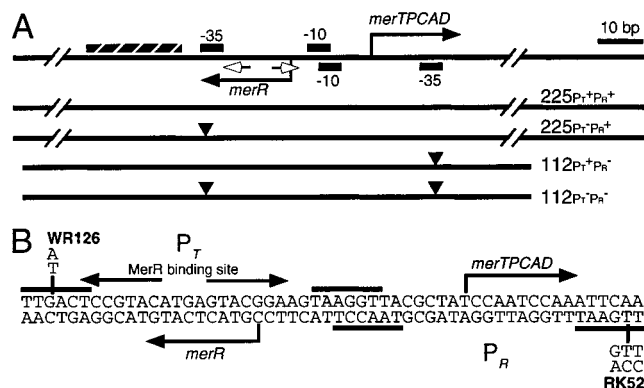


FIGURE 1: (A) Divergent Tn21 *mer* operator–promoter (*merOP*) region. Promoter elements and transcription start sites for the *merTPCAD* and for the *merR* transcripts are indicated. Outlined arrows: the dyadic MerR binding site. Stippled bar: the putative  $\alpha$  binding UP element (25). DNA templates used are shown below the map; inverted triangles indicate the mutation positions. (B) Sequence of the Tn21 *merOP*. Mutations in the  $-35$  RNAP recognition hexamer of  $P_T$  and  $P_R$  are indicated.

**Amplification of DNA Templates by PCR.** DNA templates containing WT or mutant *merOP* (Figure 1) were amplified by PCR and purified by Promega Wizard (Promega) or QIAquick (Qiagen) PCR purification kits. The 225 bp templates, 225PT<sup>+</sup>PR<sup>+</sup> and 225PT<sup>−</sup>PR<sup>+</sup>, were amplified from pWR2 and pWR126 (8), respectively. The 112PT<sup>+</sup>PR<sup>−</sup> and 112PT<sup>−</sup>PR<sup>−</sup> templates were amplified from pWR2 and pWR126, respectively, using a primer containing a mutation in the  $-35$  RNAP recognition sequence of  $P_R$  (RK52, Figure 1B), and extended from  $-77$  before *merT* to  $-52$  before *merR* transcription start sites.

**Electrophoretic Mobility Shift Assays (EMSA).** Reaction components identical to those of cross-linking reactions were incubated at 37 °C for 45 min. Heparin (final concentration 50  $\mu$ g/mL) was added, and samples were electrophoresed on 4–15% gradient polyacrylamide gels in TBE (100 mM Tris–borate, 1 mM EDTA) buffer. Ethidium bromide stained gels were scanned on a Molecular Dynamics FluorImager 575.

**Transcription Runoff Assays.** The 10  $\mu$ L reactions used the cross-linking reaction buffer described below and included 10 units of RNase inhibitor (Ambion). RNAP holoenzyme (0.5  $\mu$ M) and WT or mutant *merOP* templates (0.25  $\mu$ M) were preincubated with MerR (1  $\mu$ M) with or without HgNO<sub>3</sub> (1  $\mu$ M) for 15 min at 37 °C. Heparin (50  $\mu$ g/mL), 250  $\mu$ M each of ATP, CTP, and GTP, 100  $\mu$ M UTP, and 1  $\mu$ L of [<sup>32</sup>P]UTP (3000 Ci/mmol, 10 mCi/mL) were added, and incubation was continued for 15 min. After addition of an equal volume of loading buffer (Ambion), samples were heated at 95 °C for 3 min and loaded on 8% denaturing gels (Gene-PAGE, Amresco). Dried gels were scanned on a PhosphorImager (Molecular Dynamics). Size standards were transcribed in vitro from an RNA Century Marker Template Set (Ambion).

**Antibodies.** Polyclonal antibodies to purified MerR were raised in rabbits. Cell lines producing monoclonal anti- $\beta$  (39E4) and anti- $\beta'$  (45C6) antibodies, from J. Krakow via R. Rudner (Hunter College, SUNY), were recloned and antibodies purified. Polyclonal anti- $\alpha$  antibody was from R. Ebright (Rutgers University), and monoclonal anti- $\beta$  (originally from J. Krakow) was from Dr. T. Hoover (University

of Georgia). Anti- $\sigma^{70}$  (epitope 167–215), anti- $\beta$  (epitopes 922–1090 and 133–310, respectively), and anti- $\beta'$  (epitopes 1295–1417 and 1020–1295, respectively) were from N. Thompson (University of Wisconsin).

**Cross-Linking Reactions.** Cross-linking was done with either disuccinimidyl suberate (DSS, Pierce Chemical Co.), an amine-reactive homobifunctional cross-linker with a spacer arm of 11.4 Å (26), or with glutaraldehyde (Sigma Chemical Co.), a zero-length cross-linker which reacts with primary amines and other functional groups (27). MerR (1  $\mu$ M) and RNAP holoenzyme (0.5  $\mu$ M; Epicenter Technologies) were incubated at 37 °C for 30 min with or without one or more of the following in a 10  $\mu$ L reaction volume prior to addition of the cross-linker: wild-type (WT) or mutant *merOP* DNA (0.25  $\mu$ M), HgNO<sub>3</sub> (1  $\mu$ M; Leeman Labs), and ribonucleotides (100  $\mu$ M; Epicenter Technologies). The incubation buffer consisted of 12 mM HEPES, 12% glycerol, 5 mM MgCl<sub>2</sub>, 60 mM KCl, 0.2 mg/mL BSA, and 2 mM  $\beta$ -mercaptoethanol, pH 7.9. DSS final concentration was 0.1 mM, and glutaraldehyde final concentration was 1 mM, and the reactions were incubated at 24 °C for 15 and 30 min, respectively. Reactions were terminated by adding Laemmli's sample buffer (28), heated at 95 °C for 5 min, and electrophoresed according to Laemmli (28) on 5–15% gradient gels or 5% gels as indicated. Gels were blotted onto PVDF membranes, and Western analysis with antibodies to either MerR or a subunit of RNAP was done with the Vistra Fluorescence Western blotting kit (Amersham Life Science). Membranes were scanned on a FluorImager 575 (Molecular Dynamics) at different PMT voltages for appropriate exposures. Molecular weights were estimated based on standard protein markers (Broad range from BIO-RAD).

## RESULTS

**MerR–RNAP Assembly on *merOP* DNA.** We used EMSA to assess the assembly of preinitiation and induced complexes on WT *merOP* templates or *merOP* with mutations in either  $P_T$  or  $P_R$ . MerR bound stably to the 225 bp WT *merOP* template (M•DNA; Figure 2A, lane 2, PT<sup>+</sup>PR<sup>+</sup> panel). MerR binding was specific since MerR did not bind to a template with mutations in both *merO* dyad arms (A-28G, A-20C; 6). Also the binding of MerR to 225PT<sup>+</sup>PR<sup>+</sup> was competed by a 10-fold excess of a 31 bp template containing only the *merO* dyad and the  $-10$  and  $-35$  hexamers of  $P_T$ , but not by a 31 bp template with the *merO* dyad double mutation (data not shown).

RNAP alone bound ca. 50% of the 225 bp template containing WT  $P_T$  and  $P_R$  (PT<sup>+</sup>PR<sup>+</sup>) or mutant  $P_T$  (PT<sup>−</sup>PR<sup>+</sup>) (R•DNA band; Figure 2A, lanes 3 of respective panels) as well as the 112 bp templates containing point mutations in  $P_R$ , or in  $P_T$  and  $P_R$  (data not shown). The RNAP binding to the template with mutations in both  $P_T$  and  $P_R$  may occur because the mutations do not completely eliminate binding. The RNAP binding was stable when heparin was added last to all reactions to block nonspecific reassociation of RNAP to the DNA (29, 30). However, when heparin was added to RNAP before DNA was added, this binding was abolished (data not shown), indicating that the heparin used is active in binding to RNAP.

As in prior in vitro work (10), MerR eliminated the R•DNA bands (Figure 2A, lane 4, PT<sup>+</sup>PR<sup>+</sup> and PT<sup>−</sup>PR<sup>+</sup>

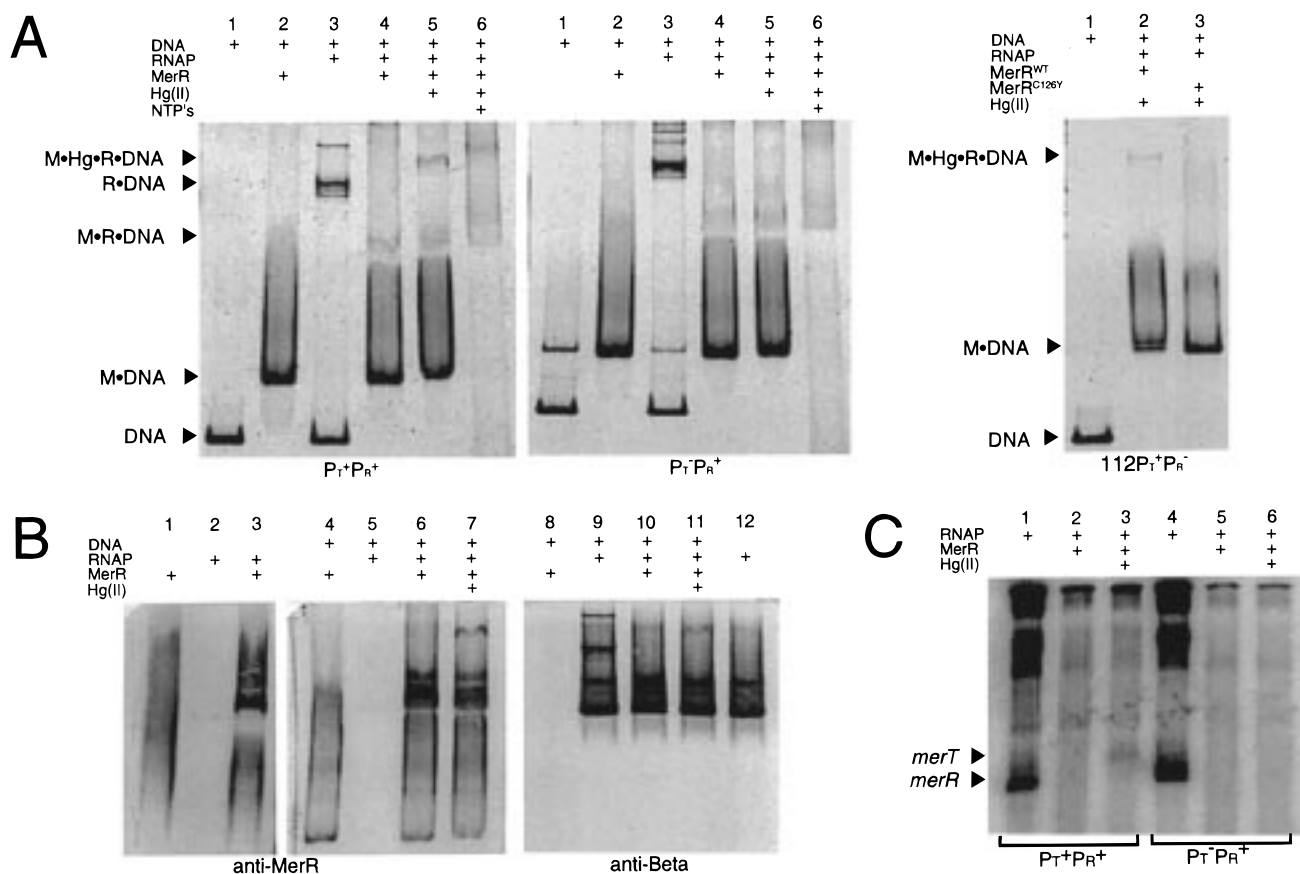


FIGURE 2: (A) EMSA of MerR(M)-RNAP(R)-DNA complexes. Reaction components were incubated at 37 °C for 45 min followed by addition of heparin (final concentration 50  $\mu$ g/mL). Samples were electrophoresed on 4–15% gradient polyacrylamide gels and stained with ethidium bromide. The extra DNA band seen in lanes 1 and 3 of the PT<sup>+</sup>PR<sup>+</sup> panel is a nonspecific artifact of PCR amplification from a supercoiled target. (B) Western analysis of EMSA gels using antibodies to either MerR or  $\beta$  as indicated. (C) Transcription runoff assays. The reaction components were incubated at 37 °C for 15 min followed by incubation with heparin and nucleotides for 15 min. Samples were electrophoresed on 8% denaturing gels. In all cases, a 225 bp template was used, except as indicated in (A) (112PT<sup>+</sup>PR<sup>-</sup>).

panels). This MerR-mediated limitation of RNAP binding to DNA occurs even with a double mutant in *merO* (pSJ255; 6) to which MerR itself does not bind (data not shown), suggesting that it arises not simply from competition for similar DNA sites, but may reflect MerR-engendered allosteric changes in RNAP itself (see below). Moreover, Western blotting of EMSA gels indicated an electrophoretically stable association between MerR and RNAP even in the absence of DNA (Figure 2B, lane 3). With MerR, a fainter but distinct band appears (Figure 2, band M•R•DNA, lane 4) which runs on EMSA within the broad MerR–RNAP band suggesting that a fraction of this band includes a M•R•DNA complex. The faster mobility of M•R•DNA compared to R•DNA complexes (Figure 2A, lanes 3 and 4, PT<sup>+</sup>PR<sup>+</sup> panel) may reflect differences in charge or DNA bending (7, 31) which this native gel system cannot discriminate. Thus, consistent with prior in vivo evidence that MerR sequesters RNAP at P<sub>T</sub> prior to induction (11), we observed a M•R•DNA ternary complex without adding the inducer Hg(II).

Addition of Hg(II) produced a very slow mobility complex (M•Hg•R•DNA; Figure 2A, lane 5, PT<sup>+</sup>PR<sup>+</sup> panel) which contained both MerR and RNAP by Western blotting (Figure 2B, lanes 7 and 11). The mutant P<sub>T</sub> did not form this Hg(II)-induced complex (Figure 2A, PT<sup>-</sup>PR<sup>+</sup> panel), indicating that the observed M•Hg•R assembled at P<sub>T</sub>. Similarly, the 112 bp templates gave rise to this M•Hg•R•DNA complex when it contained WT P<sub>T</sub> and mutant P<sub>R</sub> (lane 2 of

112PT<sup>+</sup>PR<sup>-</sup> panel), but not when it contained a mutation in both P<sub>T</sub> and P<sub>R</sub> (data not shown). Hg(II) also induced a change in the binary M•DNA complex; the M•DNA band was slightly more retarded with the 225 bp template, and a doublet band was actually seen with the 112 bp template (Figure 2A, lane 5 of PT<sup>+</sup>PR<sup>+</sup> and lane 2 of 112PT<sup>+</sup>PR<sup>-</sup> panels). MerR C126Y, which lacks one of its Hg(II) binding residues (8, 9), did not give rise to the Hg(II)-induced M•Hg•R•DNA complex or form the doublet M•DNA band (Figure 2A, lane 3, 112PT<sup>+</sup>PR<sup>-</sup> panel), confirming that both phenomena depend on Hg(II) binding by MerR. MerR C126Y, however, did bind to *merOP* DNA and destabilized the R•DNA interaction (data not shown) similar to wild-type MerR. Addition of nucleotides to the M•Hg•R•DNA complex resulted in loss of all distinct bands including the M•DNA band itself, suggesting formation of multiple DNA-bound species (Figure 2A, lane 6).

Transcriptional runoff assays done under conditions used for the EMSA and cross-linking assays (Figure 2C) demonstrated that the ternary complexes exert the expected transcriptional control at P<sub>T</sub> and P<sub>R</sub>. RNAP alone expressed predominantly the P<sub>R</sub> transcript (100 nt) either from the WT *merOP* DNA or from a P<sub>T</sub> mutant (Figure 2C, lanes 1 and 4). MerR repressed both P<sub>R</sub> and P<sub>T</sub> (105 nt) transcripts (Figure 2C, lanes 2 and 5), and with Hg(II), MerR activated expression of the P<sub>T</sub> transcript from the WT P<sub>T</sub> DNA (Figure 2C, lane 3) while it continued to repress the P<sub>R</sub> transcript.



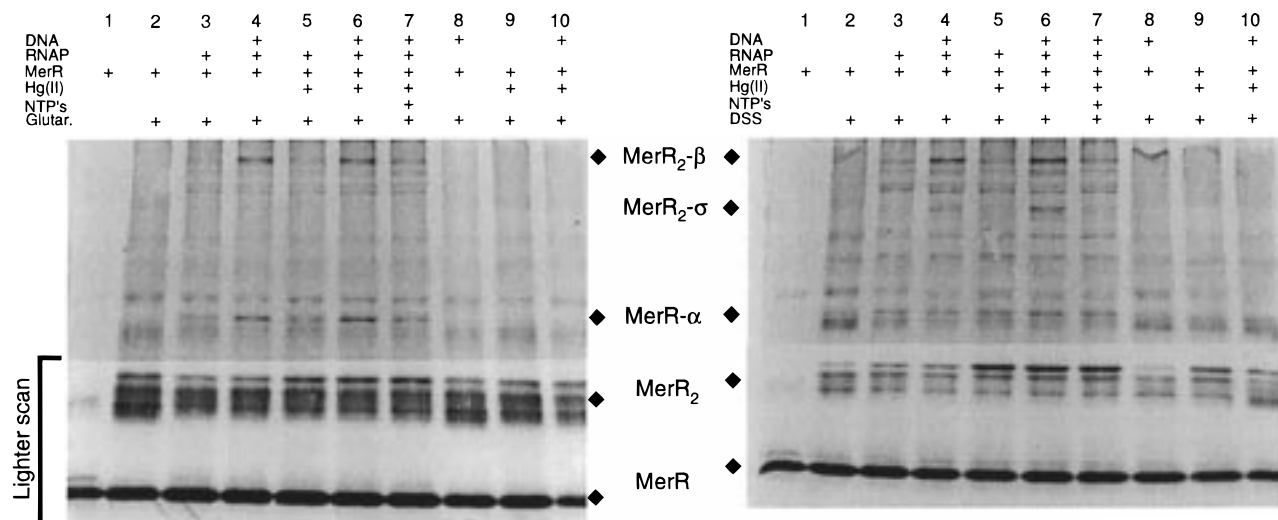


FIGURE 3: MerR cross-links to itself and to RNAP  $\alpha$ ,  $\beta$ , and  $\sigma^{70}$  subunits. Reaction components were incubated at 37 °C for 30 min followed by incubation with either glutaraldehyde (Glutar.) or DSS; reactions were run on 5–15% gradient gels and analyzed by Western blot using an anti-MerR antibody. MerR–RNAP cross-linked species were designated based on their apparent molecular weights and the reactivity with antibodies to MerR and to each RNAP subunit.

Neither transcript is produced with Hg(II) present when the template DNA carries a mutation in  $P_T$  (Figure 2C, lane 6). In addition to the expected transcripts from  $P_T$  and  $P_R$ , abundant longer transcripts (>200 nt) were observed (Figure 2C, lanes 1 and 4). Interestingly, addition of MerR largely eliminated these longer transcripts (Figure 2C, lanes 2, 3, 5, and 6). The long transcripts may originate at  $P_R$ , since they are not seen when MerR represses  $P_R$  or when  $P_R$  contains a mutation (data not shown). Their increase in length may be due to RNAP continuing around the ends of the template or hopping from one template to another. The EMSA and transcription runoff experiments demonstrated that MerR limits the occupancy of RNAP to  $P_T$  [as reported earlier; (11)]. Moreover, they showed that the complexes assembled in vitro under conditions suitable for cross-linking (albeit, not optimum for transcription) were nonetheless competent for both repression and activation by MerR.

**MerR Cross-Linked to the  $\alpha$ ,  $\beta$ , and  $\sigma^{70}$  Subunits of RNAP.** MerR cross-linked to the  $\alpha$  and  $\beta$  subunits of RNAP with glutaraldehyde and to the  $\alpha$ ,  $\beta$ , and  $\sigma^{70}$  subunits with DSS even without *merOP* DNA template (Figure 3: lane 3, both panels). These cross-links were markedly enhanced when the reaction included WT template (225PT<sup>+</sup>PR<sup>+</sup>; Figure 3, lane 4). The identity of the cross-linked MerR- $\alpha$  species (apparent molecular mass, 63 kDa; more prominent with glutaraldehyde) was confirmed by its reactivity with anti- $\alpha$  antibody (Figure 5: lanes 3 and 4). The MerR $_2$ - $\beta$  species (apparent molecular mass, 192 kDa) reacted with both anti-MerR and anti- $\beta$  antibodies and resolved more clearly on 5% gels (data not shown). The anti- $\beta'$  antibody did not react with any bands of altered mobility that were detected with the anti-MerR antibody (data not shown). The MerR $_2$ - $\sigma^{70}$  species (apparent molecular mass, 132 kDa) reacted with anti-MerR and with anti- $\sigma^{70}$  antibody (data not shown). Thus, there is a stable interaction between MerR and RNAP even when neither is bound to the DNA, and the stability of this interaction is enhanced when both are bound to DNA. MerR also cross-linked to the  $\alpha$  and  $\beta$  subunits of core RNAP alone, confirming that MerR can directly interact with core RNAP even without  $\sigma^{70}$  (data not shown). The MerR- $\alpha$  and

MerR- $\beta$  cross-links with core were less enhanced by added DNA compared to the holoenzyme cross-links, suggesting that more stable MerR–RNAP interaction is achieved by  $\sigma^{70}$ -mediated occupancy of the promoter. Hg(II) did not detectably change the MerR–RNAP cross-links regardless of whether DNA was present (Figure 3: lanes 5 and 6, both panels). Addition of nucleotides reduced the abundance of all cross-linked MerR–RNAP species (Figure 3: lane 7, both panels) to that of the “no DNA template” condition (Figure 3: lane 3, both panels), consistent with a loss of MerR–RNAP contacts upon initiation.

The MerR–RNAP cross-links were specific since the same band patterns occurred with or without 1  $\mu$ M BSA and MerR did not cross-link to BSA under these conditions (data not shown; BSA is 3  $\mu$ M in all cross-linking data presented). That MerR does not cross-link to  $\beta'$ , another large target within RNAP, is further evidence of the specificity of its interaction with the other subunits. The lower abundance of MerR–RNAP cross-linked species compared to self-cross-linked species is similar to other activator–RNAP cross-links (32, 33) and is consistent with the expectation that the MerR–RNAP cross-links would be more transient than self-interactions of either.

***merOP*-Enhancement of MerR–RNAP Cross-Links Required WT  $P_T$ .** DNA containing WT  $P_T$  and mutant  $P_R$  enhanced the MerR–RNAP cross-links (Figure 4: lane 5, both panels); DNA containing a mutation in  $P_T$  alone or in both  $P_T$  and  $P_R$  (225PT<sup>−</sup>PR<sup>+</sup>, 112PT<sup>−</sup>PR<sup>−</sup>, respectively; Figure 4, lanes 4 and 6) did not enhance the cross-links as well as the WT  $P_T$ . No enhancement occurred with a 31 bp template containing *merO* and the −10 and −35 of  $P_T$ , which binds only MerR, but not RNAP (data not shown). The implication is that MerR–RNAP cross-links enhanced by DNA arise from stable complexes assembled at  $P_T$ , and represent regulator–polymerase associations characteristic of the uninduced and induced complexes at  $P_T$ .

**Self-Cross-Linking of RNAP Subunits.** Cross-linking between the subunits of RNAP itself occurred with both reagents. The  $\alpha$  subunits of RNAP produced a homodimer (Figure 5, lane 2) which ran as two bands (estimated sizes

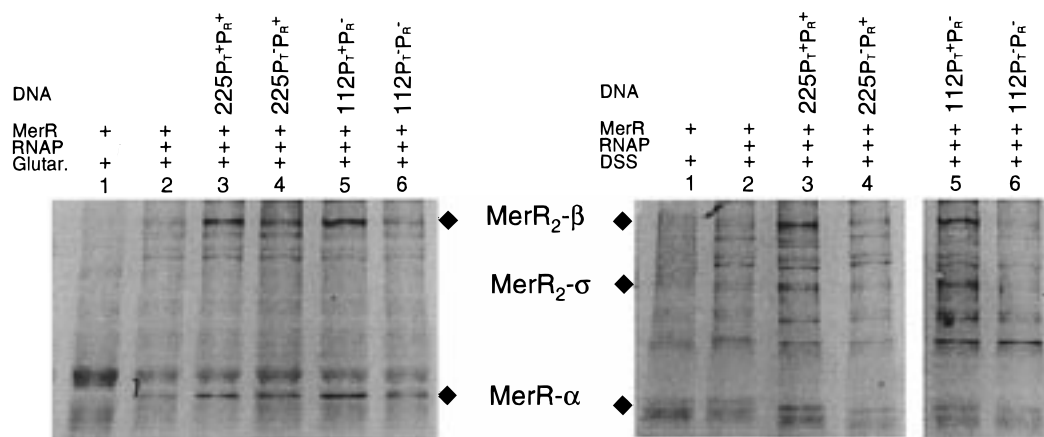


FIGURE 4: Enhancement of MerR–RNAP cross-linking by *merOP* requires  $P_T$ . Cross-linking using templates containing WT or mutant *merOP* (Figure 1) with glutaraldehyde (Glutar.) or DSS. See legend to Figure 3 for details of cross-linking reactions. In the right panel, lanes 1–4 and lanes 5–6 are results from separate experiments. Western blots were probed with antibodies to MerR.

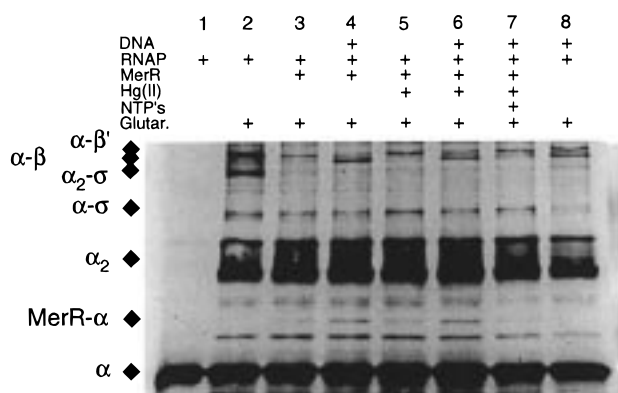


FIGURE 5: Intra-RNAP subunit cross-links. Cross-linking was done by glutaraldehyde (Glutar.); the blots were probed with anti- $\alpha$  antibody. See legend to Figure 3 for details of cross-linking reactions.

of 88 and 111 kDa), indicating that  $\alpha$  subunits cross-link as distinct conformers as previously seen (34).  $\alpha$  also cross-linked to all other subunits of RNAP, giving rise to  $\alpha$ – $\beta'$ ,  $\alpha$ – $\beta$ ,  $\alpha_2$ – $\sigma^{70}$ , and  $\alpha$ – $\sigma^{70}$  species (Figure 5, lane 2). The  $\alpha$ – $\beta'$  and  $\alpha$ – $\beta$  species ran close together on 5–15% gradient gels with apparent molecular masses of ca. 200 kDa; the  $\alpha$ – $\sigma^{70}$  and  $\alpha_2$ – $\sigma^{70}$  species were ca. 136 and 179 kDa, respectively. The same RNAP cross-linked species occurred with DSS (data not shown). Bands were identified with antibodies to  $\sigma^{70}$  and  $\beta'$  and were confirmed on 5% gels for better resolution (data not shown). The  $\alpha$ – $\beta$  band detected by anti- $\alpha$  was defined here based on its apparent molecular mass (ca. 200 kDa) and the absence of reactivity of this band with either anti- $\sigma^{70}$  or anti- $\beta'$  antibodies. Four distinct anti- $\beta$  monoclonal antibodies were used to detect the  $\alpha$ – $\beta$  band; however, all reacted weakly, making visualization of this band by the anti- $\beta$  antibody difficult (data not shown). The detection of  $\sigma$ – $\beta$ ,  $\sigma$ – $\beta'$ ,  $\beta$ – $\beta'$ , or multiple subunits cross-linked with MerR was beyond the resolution of the gel system.

**MerR and *merOP* Each Affect the Interaction of  $\alpha$  with Other RNAP Subunits.** When MerR was added to RNAP, the  $\alpha$ – $\beta'$ ,  $\alpha$ – $\beta$ , and  $\alpha_2$ – $\sigma^{70}$  species all decreased dramatically (Figure 5, lane 3), even in the absence of DNA. The WT *merOP* template alone had a different effect on RNAP self-cross-linking: both the  $\alpha_2$ – $\sigma^{70}$  and  $\alpha$ – $\beta'$  species

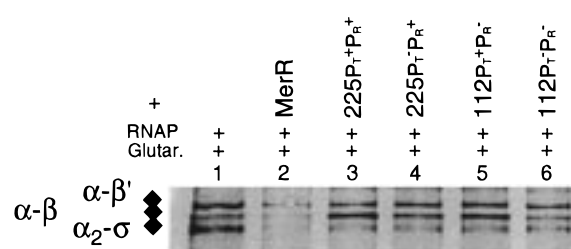


FIGURE 6: Enhancement of  $\alpha$ – $\beta$  cross-link by *merOP* requires  $P_T$ . Cross-linking with glutaraldehyde using DNA containing WT or mutant *merOP* (Figure 1). See legend to Figure 3 for details of cross-linking reactions. Western blots were probed with antibody to the  $\alpha$  subunit of RNAP.

decreased, and the  $\alpha$ – $\beta$  species increased (Figure 5, lane 8). The enhanced  $\alpha$ – $\beta$  species persisted when both MerR and DNA were mixed with RNAP (Figure 5, lane 4). Addition of Hg(II) to MerR and RNAP with or without DNA did not affect the RNAP self-cross-links (Figure 5, lane 6). Addition of nucleotides altered the relative intensities of the  $\alpha$ – $\beta'$  and the  $\alpha$ – $\beta$  species (Figure 5, lane 7) and led to a decrease of MerR– $\alpha$  (Figure 3, lane 7).

**Enhancement of  $\alpha$ – $\beta$  Cross-Links by *merOP* Required WT  $P_T$ .** With RNAP cross-linked in the presence of WT or of mutant templates, the  $\alpha_2$ – $\sigma^{70}$  and the  $\alpha$ – $\beta'$  species decreased compared to their abundance without DNA (Figure 6, lanes 3–6 compared to lane 1). However, only templates containing WT  $P_T$  (225PT<sup>+</sup>PR<sup>+</sup>, 112PT<sup>+</sup>PR<sup>–</sup>) enhanced the  $\alpha$ – $\beta$  species. Thus, interaction with  $P_T$  but not with  $P_R$  enhanced  $\alpha$ – $\beta$  cross-linked species. Intra-RNAP cross-links were not altered by a 31 bp template (covering bases –8 to –38) which binds MerR but does not bind RNAP (data not shown). The enhancement of the  $\alpha$ – $\beta$  species specifically at  $P_T$  may be due to binding of  $\alpha$ -CTD ( $\alpha$ -carboxy-terminal domain) to the UP element sequence present upstream of  $P_T$  (Figure 1; 25). With both MerR and the WT  $P_T$  (Figure 5, lane 4), the  $\alpha$ – $\beta$  cross-linking intensity more resembled that with  $P_T$  DNA alone (Figure 5, lane 8) than with MerR alone (Figure 5, lane 3), suggesting that in the MerR–RNAP–DNA complex RNAP is bound at  $P_T$ . MerR cannot interrupt this  $\alpha$ – $\beta$  association when RNAP is bound at  $P_T$  (Figure 5, lane 4).

**Self-Cross-Linking of MerR Indicates a Hg(II)-Induced Conformational Change in MerR.** As expected, since MerR

is predominantly but not exclusively a dimer at 1  $\mu$ M (9, 24), cross-linking produced abundant dimers and some higher multimers (Figure 3: lane 2, both panels). The cross-linked MerR dimer (MerR<sub>2</sub>) ran as three closely spaced cross-linked conformers with apparent molecular masses of 37, 42, and 45 kDa. Neither WT *merOP* DNA nor RNAP alone nor both together affected this dimer distribution (Figure 3: lanes 8 and 3–4, both panels). However, Hg(II) increased the abundance of the slowest mobility MerR<sub>2</sub> conformer (Figure 3, lane 9; more obvious with DSS), regardless of whether DNA was present (Figure 3, lane 10). This Hg(II)-induced change in the MerR<sub>2</sub> conformer distribution was even more prominent with RNAP present, with or without DNA (Figure 3: lanes 5 and 6, both panels) and did not occur with the Hg(II) binding mutant C126Y (data not shown; 8, 9).

## DISCUSSION

**Stable MerR Associations with RNAP.** Our recent finding of MerR-specific effects of mutations in both *rpoA* and *rpoD* (23) suggested that  $\alpha$  as well as  $\sigma^{70}$  might contact MerR at some stage of transcriptional initiation. No prior work had specifically implicated interactions between MerR and the two large polymerase subunits,  $\beta$  and  $\beta'$ . In the work presented here, MerR–RNAP interactions are demonstrated by MerR–RNAP cross-links in the absence of DNA, by alteration of RNAP self-cross-linking by MerR, and by an electrophoretically stable association between MerR and RNAP (Figures 3, 5, and 2B, lane 3 of each figure).

MerR cross-linked to the  $\alpha$ ,  $\beta$ , and  $\sigma^{70}$  subunits of RNAP even in the absence of promoter DNA (Figure 3, lane 3), indicating that MerR alone contacts RNAP stably enough for the cross-linking to occur. These contacts were enhanced in functional MerR–RNAP complexes assembled at P<sub>T</sub> (Figure 3, lane 4; Figure 4, lanes 3 and 5). MerR cross-links to the  $\alpha$  and  $\beta$  subunits of the RNAP core as well as the holoenzyme (Figure 3, lanes 3 and 4, and data not shown). This indicates that MerR interacts with both RNAP core as well as holoenzyme, even though these two forms of RNAP have significant conformational differences (35). The constancy of MerR–RNAP cross-links on exposure to Hg(II) indicates that MerR maintains similar, although not necessarily identical, associations with RNAP subunits during both activation and repression. An analogous finding has been made with the bacteriophage  $\phi$ 29 regulator protein p4 in which the same residues are involved in both repression and activation, at the A2c and late A3 promoters, respectively (36).

Growing evidence from many systems underscores the utility of cross-linking in revealing areas of functional relevance in interacting proteins (32, 33, 37, 38). The number and variety of MerR's cross-links with RNAP subunits are unprecedented among regulatory proteins and are consistent with more extensive surface proximity between RNAP and MerR than any previously described prokaryotic transcriptional regulator. Other regulators interact with either one (29, 33, 36, 37, 39–45) or two subunits of RNAP (32, 38, 46), with the  $\alpha$  and the  $\sigma$  subunits being the most common targets.

Our observations also indicate remodeling by MerR and by *merOP* of contacts between the RNAP subunits themselves as suggested by alterations in the  $\alpha$ – $\beta$ ,  $\alpha$ – $\beta'$ , and  $\alpha$ – $\sigma^{70}$  cross-links (Figure 5, lanes 3 and 8). The  $\alpha$  and  $\sigma^{70}$

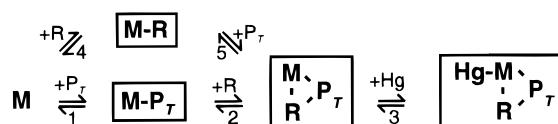


FIGURE 7: Complexes involved in transcriptional control of the *mer* operon. M, MerR; P<sub>T</sub>, *merTPCAD* promoter DNA; R, RNAP; Hg, Hg(II). Numbers refer to steps in the process elaborated in the text.

subunits stably contact the larger subunits,  $\beta$  and  $\beta'$  (47, 48), and  $\sigma^{70}$  has close proximity to the  $\alpha$ -CTD (49). No prior work has examined the effects of either promoter DNA or a regulatory protein on RNAP self-cross-links. The MerR-mediated losses of the  $\alpha$ – $\beta$  and  $\alpha$ – $\beta'$  cross-links were most unexpected as association of  $\alpha$ ,  $\beta$ , and  $\beta'$  is the foundation of core polymerase. It is unlikely that MerR interposes extensively between  $\alpha$  and  $\beta$  or  $\beta'$ . A probable participant in at least some of these MerR-interrupted RNAP self-cross-links is the highly mobile  $\alpha$ -CTD (50). That MerR interfered with  $\alpha$ 's contacts to  $\beta'$ , the only subunit to which MerR did not itself cross-link, further suggests that MerR interacts with the  $\alpha$ -CTD which might contact  $\beta'$  in the absence of DNA. This is also suggested by disruption of  $\alpha_2$ – $\sigma^{70}$  by MerR since  $\alpha_2$ – $\sigma^{70}$  contacts might also involve the flexible CTD of at least one  $\alpha$  monomer (49). Alternatively, MerR might cause conformational changes in  $\alpha$  and/or  $\sigma^{70}$  which affect the stability of their interactions indirectly.

**Model for *mer* Regulation.** Our findings are integrated with previous knowledge of *mer* transcriptional regulation in Figure 7. Reactions 1 through 3 depict complexes of the *mer* transcription control components in the order we expect they occur in vivo at WT P<sub>T</sub>. Since MerR has a high affinity for DNA (10, 18), in vivo, it binds stably to DNA (Figure 7, reaction 1) to form the repressed complex M–P<sub>T</sub> (11, 13, 14). With MerR bound, RNAP binds preferentially to P<sub>T</sub> (Figure 7, reaction 2), leading to formation of the uninduced ternary closed complex (M–P<sub>T</sub>–R). In vitro we found that MerR and RNAP bind to *merOP* independently. However, the elimination by MerR of RNAP-generated slow mobility DNA bands in EMSA (Figure 2A, lane 4, PT<sup>+</sup>PR<sup>+</sup> panel) and of non-P<sub>T</sub> transcripts (Figure 2C, lanes 2 and 5) suggests that MerR alters RNAP so as to limit its occupancy to P<sub>T</sub>. The assembly of MerR and RNAP at P<sub>T</sub> is also suggested by enhanced cross-links between MerR and RNAP specifically mediated by WT P<sub>T</sub> DNA (Figure 4, lanes 3 and 5). The same cross-links between MerR and RNAP bound on the DNA pre- and post-Hg(II) addition demonstrate for the first time in vitro the unusual behavior of MerR, i.e., capture of RNAP at P<sub>T</sub> even in the absence of the inducer Hg(II) as previously demonstrated in vivo (11, 13, 14). The physical basis for MerR's ability to sequester RNAP in a preinitiation complex at P<sub>T</sub> (11) may lie in stable associations with three of the four subunits of RNAP holoenzyme. Hg(II)-induced allosteric changes in MerR which lead to underwinding of *merOP* (11, 12, 14, 15, 51) were here demonstrated by marked alteration in the MerR dimer conformation (Figure 3, lanes 9, 5–7), by the doublet MerR–DNA band (Figure 2A, lane 2, 112PT<sup>+</sup>PR<sup>+</sup> panel), and by formation of a distinct very slow mobility complex in EMSA (Figure 2A, lane 5 of PT<sup>+</sup>PR<sup>+</sup> panel; Figure 2B, lanes 7 and 11). In the activated complex (Hg–M–P<sub>T</sub>–R, Figure 7), MerR still maintains its contacts with RNAP (Figure 3, lane 6). Reaction 4 represents



an interaction between MerR and RNAP (Figure 7, M–R) when neither is bound to DNA, observed here in vitro for the first time.

In summary, our work reveals that MerR associates specifically with RNAP even without DNA. These associations are markedly stabilized by binding to  $P_T$  at which MerR normally operates. Previously, MerR-mediated activation has been attributed primarily to DNA underwinding by MerR; our findings provide a new look at the mechanism, implicating MerR–RNAP interactions during both active repression and Hg(II)-induced activation. Current efforts are directed at quantifying the equilibrium constants of these interactions and identifying the precise residues involved in the interactions.

## ACKNOWLEDGMENT

We thank T. Hoover for cross-linking guidance, R. H. Ebright, T. Hoover, and N. Thompson for antibodies to RNAP subunits, R. Rudner and J. Krakow for monoclonal antibody cell lines, and Q. Zeng for C126Y protein. We also appreciate helpful criticism of the manuscript from L. Caslake, A. Dombroski, T. Hoover, C. Moran, and W. Ross.

## REFERENCES

- Hochschild, A., and Dove, S. L. (1998) *Cell* 92, 597–600.
- Fassler, J. S., and Gussin, G. N. (1996) *Methods Enzymol.* 273, 3–29.
- Summers, A. O. (1992) *J. Bacteriol.* 174, 3097–3101.
- O'Halloran, T. V., and Walsh, C. (1987) *Science* 235, 211–214.
- Heltzel, A., Gambill, D., Jackson, W. J., Totis, P. A., and Summers, A. O. (1987) *J. Bacteriol.* 169, 3379–3384.
- Park, S.-J., Wireman, J., and Summers, A. O. (1992) *J. Bacteriol.* 174, 2160–2171.
- Ansari, A. Z., Chael, M. L., and O'Halloran, T. V. (1991) *Nature* 355, 87–89.
- Ross, W., Park, S.-J., and Summers, A. O. (1989) *J. Bacteriol.* 171, 4009–4018.
- Shewchuk, L. M., Helmann, J. D., Ross, W., Park, S. J., Summers, A. O., and Walsh, C. T. (1989) *Biochemistry* 28, 2340–2344.
- O'Halloran, T. V., Frantz, B., Shin, M. K., Ralston, D. M., and Wright, J. G. (1989) *Cell* 56, 119–129.
- Heltzel, A., Lee, I. W., Totis, P. A., and Summers, A. O. (1990) *Biochemistry* 29, 9572–9584.
- Frantz, B., and O'Halloran, T. V. (1990) *Biochemistry* 29, 4747–4751.
- Lee, I. W., Livrelli, V., Park, S.-J., Totis, P. A., and Summers, A. O. (1993) *J. Biol. Chem.* 268, 2632–2639.
- Livrelli, V., Lee, I. W., and Summers, A. O. (1993) *J. Biol. Chem.* 268, 2623–2631.
- Ansari, A. Z., Bradner, J. E., and O'Halloran, T. V. (1995) *Nature* 374, 371–375.
- Helmann, J. D., Wang, Y., Mahler, I., and Walsh, C. T. (1989) *J. Bacteriol.* 171, 222–229.
- Parkhill, J., Ansari, A. Z., Wright, J. G., Brown, N. L., and O'Halloran, T. V. (1993) *EMBO J.* 12, 413–421.
- Shewchuk, L. M., Verdine, G. L., and Walsh, C. T. (1989) *Biochemistry* 28, 2331–2339.
- Condee, C. W., and Summers, A. O. (1992) *J. Bacteriol.* 174, 8094–8101.
- Cowell, I. G. (1994) *Trends Biochem. Sci.* 19, 38–42.
- Fondell, J. D., Roy, A. L., and Roeder, R. G. (1994) *Genes Dev.* 7, 1400–1410.
- Comess, K. M., Shewchuk, L. M., Ivanetich, K., and Walsh, C. T. (1994) *Biochemistry* 33, 4175–4186.
- Caslake, L. F., Ashraf, S. I., and Summers, A. O. (1997) *J. Bacteriol.* 179, 1787–1795.
- Zeng, Q., Staalhandske, C., Anderson, M. C., Scott, R. A., and Summers, A. O. (1998) *Biochemistry* 37, 15885–15895.
- Ross, W., Aiyar, S. E., Salomon, J., and Gourse, R. L. (1998) *J. Bacteriol.* 180, 5375–5383.
- Mattson, G., Conklin, E., Desai, S., Nielander, G., Savage, M. D., and Morgensen, S. (1993) *Mol. Biol. Rep.* 17, 167–183.
- Habeeb, A. F. S. A., and Hiramoto, R. (1968) *Arch. Biochem. Biophys.* 126, 16–26.
- Laemmli, U. K. (1970) *Nature* 227, 680–685.
- Choy, H. E., Park, S. W., Aki, T., Parrack, P., Fujita, N., Ishihama, A., and Adhya, S. (1995) *EMBO J.* 14, 4523–4529.
- Straney, S. B., and Crothers, D. M. (1987) *Biochemistry* 26, 5063–5070.
- Record, M. T., Reznikoff, W. S., Craig, M. L., McQuade, K. L., and Schlax, P. J. (1996) in *Escherichia coli and Salmonella: Cellular and Molecular Biology* (Neidhardt, F. C., Ed.) pp 792–820. ASM Press, Washington, D.C.
- Lee, J. H., and Hoover, T. R. (1995) *Proc. Natl. Acad. Sci. U.S.A.* 92, 9702–9706.
- Miller, A., Wood, D., Ebright, R. H., and Rothman-Denes, L. B. (1997) *Science* 275, 1655–1657.
- Hillel, Z., and Wu, C. (1977) *Biochemistry* 16, 3334–3342.
- Polyakov, A., Severinova, E., and Darst, S. A. (1995) *Cell* 83, 365–373.
- Monsalve, M., Mencia, M., Rojo, F., and Salas, M. (1996) *EMBO J.* 15, 383–391.
- Chen, Y., Ebright, Y. W., and Ebright, R. H. (1994) *Science* 265, 90–92.
- Jin, R., Sharif, K. A., and Krakow, J. S. (1995) *J. Biol. Chem.* 270, 19213–19216.
- Bokal, A. J., Ross, W., Gaal, T., Johnson, R. C., and Gourse, R. L. (1997) *EMBO J.* 16, 154–162.
- Kuldell, N., and Hochschild, A. (1994) *J. Bacteriol.* 176, 2991–2998.
- Landini, P., Bown, J. A., Volkert, M. R., and Busby, S. J. W. (1998) *J. Biol. Chem.* 273, 13307–13312.
- Li, M., Moyle, H., and Susskind, M. M. (1994) *Science* 263, 75–77.
- Makino, K., Amemura, M., Kim, S. K., Nakata, A., and Shinagawa, H. (1993) *Genes Dev.* 7, 149–160.
- Niu, W., Kim, Y., Tau, G., Heyduk, T., and Ebright, R. H. (1996) *Cell* 87, 1123–1134.
- Szalewska-Palasz, A., Wegrzyn, A., Blaszcak, A., Taylor, K., and Wegrzyn, G. (1998) *Proc. Natl. Acad. Sci. U.S.A.* 95, 4241–4246.
- Artsimovitch, I., Murakami, K., Ishihama, A., and Howe, M. M. (1996) *J. Biol. Chem.* 271, 32343–32348.
- Greiner, D. P., Hughes, K. A., Gunasekera, A. H., and Meares, C. F. (1996) *Proc. Natl. Acad. Sci. U.S.A.* 93, 71–75.
- Heyduk, T., Heyduk, E., Severinov, K., Tang, H., and Ebright, R. H. (1996) *Proc. Natl. Acad. Sci. U.S.A.* 93, 10162–10166.
- McMahan, S. A., and Burgess, R. R. (1994) *Biochemistry* 33, 12092–12099.
- Blatter, E. E., Ross, W., Tang, H., Gourse, R. L., and Ebright, R. H. (1994) *Cell* 78, 889–896.
- Helmann, J. D. (1997) in *Metal Ions in Gene Regulation* (Walden, W. E., and Silver, S., Eds.) pp 45–76, Chapman & Hall, London.

BI982814M